

NIST-GCR-98-756

**ANALYSIS OF THE ISO 9705 ROOM/CORNER
TEST: SIMULATIONS, CORRELATIONS AND
HEAT FLUX MEASUREMENTS**

**Scott Edward Dillon
University of Maryland
College Park, MD 20742**



**United States Department of Commerce
Technology Administration
National Institute of Standards and Technology**

**ANALYSIS OF THE ISO 9705 ROOM/CORNER
TEST: SIMULATIONS, CORRELATIONS AND
HEAT FLUX MEASUREMENTS**

Prepared for
U.S. Department of Commerce
National Institute of Standards and Technology
Gaithersburg, MD 20899

By
Scott Edward Dillon
University of Maryland
College Park, MD 20742

August 1998



Notice

This report was prepared for the Building and Fire Research Laboratory of the National Institute of Standards and Technology under grant number 60NANB2D1266. The statement and conclusions contained in this report are those of the authors and do not necessarily reflect the views of the National Institute of Standards and Technology or the Building and Fire Research Laboratory.

ANALYSIS OF THE ISO 9705 ROOM/CORNER TEST:
SIMULATIONS, CORRELATIONS AND HEAT FLUX MEASUREMENTS

by

Scott Edward Dillon

Thesis submitted to the Faculty of the Graduate School of the
University of Maryland, College Park in partial fulfillment
of the requirements for the degree of
Master of Science
1998

Advisory Committee:

Professor James G. Quintiere
Dr. Frederick W. Mowrer
Dr. Jose Torero

ABSTRACT

Title of Thesis: AN ANALYSIS OF THE ISO 9705 ROOM-CORNER
TEST: SIMULATIONS, CORRELATIONS AND
HEAT FLUX MEASUREMENTS

Degree Candidate: Scott Edward Dillon

Degree and Year: Master of Science in Fire Protection Engineering, 1998

Thesis Directed by: Professor James Quintiere
Fire Protection Engineering

A simulation model is implemented in order to predict the fire performance of materials in the ISO 9705 Room-Corner Test. These materials were tested by the L S Fire Laboratories of Italy, and the data they provided is analyzed in this report. A method was established to define material properties including the heat of combustion, heat of gasification, thermal inertia, ignition temperature and the total energy released per unit area. These methods were developed from refinements in a theoretical model of ignition and in resolving time dependent effects in the Cone Calorimeter. The materials examined consist of some of the most difficult to analyze because they melt, drip, expand and de-laminate from the wall and ceiling configuration of the room-corner test. Corrections have been included in the simulation modeling to account for these effects. The correction involves reducing the total energy content per unit area

of the material to accordingly reduce its contribution as a wall-ceiling oriented element. An empirical correlation based on a linearized upward flame spread model is shown to provide excellent comparison to the flashover time in the full-scale ISO test. Accurate heat flux measurements from the ignition burner at an energy release of 100 and 300 kW were made from full-scale room-corner tests. Corrections to these heat flux measurements provide the incident heat flux from the burner fire plume and from a combination of the plume and the thermal feedback of the heated room. Detailed heat flux distributions along the walls and ceiling in the vicinity of the ignition burner are provided.

ACKNOWLEDGEMENTS

I am incredibly grateful to Silvio Messa and the entire staff of the L S Fire Laboratories, Moutano, Italy. Their contributions to this project have been enormous and have increased its value and accuracy beyond what we could have possibly achieved separately. I am also indebted to NIST/BFRL for their financial support and to Dr. Thomas Ohlemiller for his technical guidance. I also want to thank Dr. Mowrer and Dr. Torero for serving on my committee as well as the entire staff of the Fire Protection Engineering department for being such a great help and putting up with me for so long.. In conclusion I want to thank Dr. James G. Quintiere. Working under his tutelage has been an incredibly rewarding and thought provoking experience... quite simply, he's the man!

TABLE OF CONTENTS

LIST OF TABLES	vii
LIST OF FIGURES	ix
1. INTRODUCTION	1
1.1 Room-Corner Tests	1
1.2 Modeling	3
2. DESCRIPTION OF MATERIALS	7
3. DETERMINING MATERIAL PROPERTIES	13
3.1 Ignition Properties	14
3.2 Flame Spread Properties	16
3.3 Heat of Combustion (ΔH_C)	18
3.3.1 Definition	18
3.3.2 Determining ΔH_C	19
3.3.2.1 Peak Rate of Energy Release ($\Delta H_{C, peak}$)	22
3.3.2.2 Average Rate of Energy Release ($\Delta H_{C, peak avg.}$)	23
3.3.2.3 Overall Energy Release ($\Delta H_{C, overall avg.}$)	25
3.4 Heat of Gasification (L)	26
3.4.1 Definition	26
3.4.2 Cone Calorimeter Heat Flux	29
3.4.3 Energy Release Rate Methods	34
3.4.3.1 Peak Energy Release Rate (L_{peak})	35
3.4.3.2. Average Energy Release Rate Around the Peak ($L_{peak avg.}$)	36
3.4.3.3. Average Overall Test Results ($L_{overall avg.}$)	36
3.4.4 Specimen Mass Loss Methods	39
3.4.4.1 Peak Energy Release Rate (L_{peak}) by Mass Loss	40
3.4.4.2 Average Energy Release Rate Around the Peak ($L_{peak avg.}$) by Mass Loss	41
3.4.4.3 Average Overall Test Results ($L_{overall avg.}$) by Mass Loss	41
3.4.5 Heat of Gasification Value Analysis	41
3.5 Total Energy Per Unit Area (Q'')	48
3.6 Material Property Conclusion	50
4. FIRE GROWTH PREDICTIONS	53
4.1 Fire Growth Model	53

4.2 Material Properties Used	55
4.2.1 Adjusted Properties for Melting/Dripping Materials.....	56
4.3 Results	59
4.3.1 R 4.01, Fire Retarded Chipboard.....	62
4.3.2 R 4.02 Paper Faced Gypsum Board.....	63
4.3.3 R 4.03 Polyurethane Foam Panel with Aluminum Facing.....	64
4.3.4 R 4.05, Fire Retarded Extruded Polystyrene Board	67
4.3.5 R 4.06, Clear Acrylic Glazing	68
4.3.6 R 4.07, Fire Retarded PVC	70
4.3.7 R 4.08, 3-Layered, Fire Retarded Polycarbonate Panel.....	72
4.3.8 R 4.09, Varnished Massive Timber	73
4.3.9 R 4.10, Fire Retarded Plywood	75
4.3.10 R 4.11, Normal Plywood.....	76
4.3.11 R 4.20, Fire Retarded Expanded Polystyrene Board (40 mm)	77
4.3.12 R 4.21, Fire Retarded Expanded Polystyrene Board (80 mm)	79
4.3.13 Time to Reach Flashover.....	81
4.4 Lateral Flame Spread.....	83
4.5 Large-Scale Room Fire Experiments	83
5. FIRE GROWTH CORRELATION	90
5.1 Upward Flame Spread Acceleration Factor.....	90
5.2 Burnout Time Considerations.....	94
6. IGNITION BURNER FLAME HEIGHT AND HEAT FLUX.....	99
6.1 Flame Height.....	100
6.1.1 Open Corner	100
6.1.1.1 Hasemi and Tokunaga.....	102
6.1.1.2 Kokkala	102
6.1.1.3 Revised Heskestad Correlation.....	103
6.1.1.4 Janssens	104
6.1.1.5 Comparison of Corner-Flame Height Determinations.....	105
6.1.2 Ceiling Jets	106
6.2 Heat Flux.....	108
6.2.1 Kokkala	108
6.2.2 Janssens.....	109
6.2.3 Conclusion.....	110

7. SMALL-SCALE STEEL PLATE VALIDATION.....	111
7.1 Experiments by Ingason and de Ris	111
7.2 Experimental Set-Up and Procedure	112
7.3 Heat Transfer Analysis	117
7.3.1 Conduction—Steel Plate	118
7.3.2 Conduction—Insulation	122
7.3.3 Convection.....	123
7.3.4 Re-Radiation.....	128
7.3.5 Energy Storage Term	129
7.4 Incident Heat Flux Equation	131
7.5 Small-Scale Steel Plate Test Results	132
8. FULL-SCALE HEAT FLUX MEASUREMENTS	140
8.1 Test Configuration.....	140
8.1.1 Steel Plate Assembly.....	140
8.1.2 Plate Mounting	142
8.1.3 Ignition Source	143
8.1.4 Thermocouples	146
8.1.5 Heat Flux Meters	146
8.1.6 Exhaust Hood	147
8.1.7 Data Acquisition System.....	148
8.2 Test Procedure	148
8.3 Heat Transfer Analysis	149
8.3.1 Total Measured Heat Flux.....	149
8.3.2 Conduction Losses Through Insulation	151
8.3.3 Cold Surface Correction Factor.....	152
8.3.4 Heated Room Effect.....	155
8.4 Full-Scale Test Results	158
8.4.1 Heat Flux.....	159
8.4.2 Flame Length.....	170
8.4.3 Plume Approximations	174
9. CONCLUSIONS.....	176
APPENDIX – Calculated Heat Flux Tables and Distributions.	179

REFERENCES	192
------------------	-----

LIST OF TABLES

Table 3. 1: Material Modeling Properties.	13
Table 3. 2: Estimated Critical Heat Flux for Ignition	16
Table 3. 3: Ignition and Flame Spread Properties of the LSF Materials.....	18
Table 3. 4: Average, Effective Heat of Combustion (ΔH_c) Values Calculated by Three Methods.	26
Table 3. 5: Effective Heat of Gasification (L) Values Calculated by Six Methods.....	42
Table 3. 6: Total Energy per Unit Area of Material.....	49
Table 4. 1: Ignition, Flame Spread and Energy Release Properties of the LSF Materials used for Modeling.	61
Table 4. 2: Comparison of the Time to Reach Flashover (1,000 kW) for the Full-Scale Room-corner Tests and the Model Predictions.....	82
Table 4. 3: Ignition, Flame Spread and Energy Release Properties of the EUREFIC Materials.	85
Table 5. 1: Fire Growth Correlation Parameters for Swedish, EUREFIC and LSF Materials.	53
Table 6. 1: Dimensionless Energy Release Rate Parameters for Different Burner Sizes and Energy Output Levels.	101
Table 6. 2: Flame Height for 17 and 30 cm Square Ignition Burners at 40 to 300 kW Energy Release Rates, Calculated by Janssens [23].	105
Table 6. 3: Incident Heat Flux to the Corner from 17 and 30 cm Square Ignition Burners at 40 to 300 kW Energy Release Rates, Calculated by Janssens [23].	110
Table 8. 1: Propane Flow Rates Used in the Room/Corner Test.....	146
Table 8. 2: Percentage of Incident Heat Flux Lost to the Ceramic Fiber Insulation – Small Scale Plate Testing.	152
Table 8. 3: Average Fire Plume and Equilibrium Heat Fluxes for 100 and 300 kW Burners Measured with Water Cooled Schmidt-Boelter Heat Flux Meters.	166
Table 8. 4: Minimum, Maximum and Average Flame Lengths for the 0.17 m Burner in the Corner of the ISO 9705 Standard Room: 100 and 300 kW.	172

Table 8. 5: Calculated and Experimentally Observed Flame Heights for 100 and 300 kW Heat Release Rates Using a 0.17 m Square Burner in the Standard ISO Test Room.....	173
--	-----

LIST OF FIGURES

Figure 1. 1: Schematic Drawing of the ISO 9705 Room-Corner Test [49].	10
Figure 3. 1: Typical Interpretive Plot of Ignition Data in Order to Derive Properties: R 4.21, Fire Retarded Expanded Polystyrene Board.	10
Figure 3. 2: A Typical Burning Process in the Roland Apparatus	10
Figure 3. 3: Example of Time-Varying Heat of Combustion Measured in the Cone Calorimeter: R 4.08, 3-Layer Polycarbonate Panel at 50 kW/m ² in the Cone Calorimeter.	10
Figure 3. 4: Example of Peak, Peak Average and Overall Average Energy Release Rates per Unit Area Measured in the Cone Calorimeter: R 4.08 at 50 kW/m ² in the Cone.	10
Figure 3. 5: Method of Determining the Peak, Peak Average and Overall Average Heat of Combustion Values: R 4.08, 3-Layer Polycarbonate Panel at 50 kW/m ² in the Cone Calorimeter.....	10
Figure 3. 6: Example of a Typical Average Heat of Combustion ($\overline{\Delta H_c}$) Determination: R 4.08 at 50 kW/m ²	10
Figure 3. 7: Example of a Typical Burning Rate per Unit Area (\dot{m}'') Prediction: R 4.08, 3-Layer Polycarbonate Panel at 50 kW/m ² in the Cone Calorimeter.....	10
Figure 3. 8: Example of a Typical Energy Release Rate per Unit Area (\dot{Q}'') Prediction: R 4.08, 3-Layer Polycarbonate Panel at 50 kW/m ² in the Cone Calorimeter.	10
Figure 3. 9: Example of a Typical Heat of Gasification (L) Determination Using Energy Release Rates per Unit Area with Respect to the External Heat Flux in the Cone Calorimeter: R 4.05, Fire Retarded Extruded Polystyrene.....	10
Figure 3. 10: Example of Steady Burning Rate (\dot{m}) Determination: R 4.08, 3-Layer Polycarbonate Panel.	10
Figure 3. 11: Example of a Typical Heat of Gasification (L) Determination Using Specimen Mass Loss Rates per Unit Area with Respect to the External Heat Flux in the Cone Calorimeter: R 4.05, Fire Retarded Extruded Polystyrene.....	10
Figure 3. 12: Typical Energy Release Rate per Unit Area and Specimen Mass for Gypsum Board, R 4.02, in the Cone Calorimeter.	10
Figure 3. 13: Typical Energy Release Rate and Specimen Mass for Polyurethane Foam Board with Paper Facing, R 4.04, in the Cone Calorimeter.	10

Figure 3. 14: Average Heat of Combustion Values for Fire Retarded PVC, R 4.07.....	45
Figure 3. 15: Various Energy Release Rates for Fire Retarded PVC, R 4.07, in the Cone Calorimeter	46
Figure 3. 16: Peak Energy Release and Mass Loss Rates for Varnished Massive Timber, R 4.09, at Different External Heat Flux Levels in the Cone Calorimeter.	46
Figure 3. 17: Typical Total Energy per Unit Area (Q'') Determination: R 4.05, Extruded Polystyrene Board.	49
Figure 3. 18: Comparison of Methods for Predicting the Energy Release Rate of a Thermoplastic Material in the Cone Calorimeter: R 4.08, 3-Layer Polycarbonate Panel at 50 kW/m ²	51
Figure 3. 19: Comparison of Methods for Predicting the Energy Release Rate of a Charring Material in the Cone Calorimeter: R 4.11, Normal, Untreated Plywood at 50 kW/m ²	52
Figure 4. 1: Features of Quintiere's Fire Growth Model.	55
Figure 4. 2: Idealized Heat Flux Distributions Used in Quintiere's Fire Growth Model.	58
Figure 4. 3: Full-Scale Energy Release Rate for Fire Retarded Chipboard, R 4.01.....	63
Figure 4. 4: Full-Scale Energy Release Rate for Paper Faced Gypsum Board, R 4.02. 64	
Figure 4. 5: Full-Scale Energy Release Rate for Polyurethane Foam Panel with Aluminum Facing, R 4.03, Using Material Properties for Polyurethane Panel with Paper Facing, R 4.04.....	66
Figure 4. 6: Full-Scale Energy Release Rate for Extruded Polystyrene Board, R 4.05..	68
Figure 4. 7: Full-Scale Energy Release Rate for Acrylic Glazing, R 4.06.....	70
Figure 4. 8: Full-Scale Energy Release Rate for R 4.07 Fire Retarded PVC.....	72
Figure 4. 9: Full-Scale Energy Release Rate for 3-Layered, Fire Retarded Polycarbonate Panel, R 4.08.	74
Figure 4. 10: Full-Scale Energy Release Rate for Varnished Massive Timber, R 4.09.	75
Figure 4. 11: Full-Scale Energy Release Rate for Fire Retarded Plywood, R 4.10.....	76
Figure 4. 12: Full-Scale Energy Release Rate for Normal Plywood, R 4.11.....	77
Figure 4. 13: Full-Scale Energy Release Rate for Fire Retarded Expanded Polystyrene Board (40 mm), R 4.20.....	79
Figure 4. 14: Full-Scale Energy Release Rate for Fire Retarded Expanded Polystyrene Board (80 mm), R 4.21.....	81

Figure 4. 15: Large-Scale Test Ignition Burner Used by Kokkala <i>et. al.</i>	84
Figure 4. 16: Large-Scale Energy Release Rate for Textile Wall Covering on Gypsum Board.	87
Figure 4. 17: Large-Scale Energy Release Rate for Combustible Facing on Mineral Wool.	87
Figure 4. 18: Large-Scale Energy Release Rate for Fire Retarded Particle Board, Type B1.	88
Figure 4. 19: Large-Scale Energy Release Rate for Ordinary Birch Plywood.....	88
Figure 4. 20: Large-Scale Energy Release Rate for PVC Wall Covering on Gypsum Board.	89
Figure 5. 1: Time to Flashover as a Function of the Flame Spread Acceleration Factor.	93
Figure 5. 2: Dimensionless Time as a Function of the Flame Spread Acceleration Factor.....	94
Figure 5. 3: Small Dimensionless Burnout Time [$\tau_{fo} > (\tau_b + 1)$], $\tau_{fo} - 1 - \tau_b$ versus b	96
Figure 5. 4: Large Dimensionless Burnout Time [$\tau_{fo} \leq (\tau_b + 1)$], $\tau_{fo} - 1$ versus a	97
Figure 6. 1: Corner Burner Configurations.	101
Figure 6. 2: Flame Temperature Distributions 3 cm from the Wall for a 17 cm x 17 cm Burner at 100 kW and a 30 cm x 30 cm Burner at 160 kW [26].	104
Figure 6. 3: Dimensionless Average Flame Height (Z_f/D) in a Corner as a Function of the Dimensionless Energy Release (Q^*).	106
Figure 6. 4: Horizontal Flame Lengths Under a Ceiling From a Corner Ignition Burner [48].	108
Figure 6. 5 (a & b): Heat Flux Distributions to the Wall from a 17 cm x 17 cm Propane Gas Burner Located in the Corner with Energy Release Rates of 100 and 300 kW [26, 27].	109
Figure 7. 1: Small-Scale Steel Plate Thermocouple Geometry.	113
Figure 7. 2 Small-Scale ,Steel Plate LIFT Apparatus Test Assembly (Exploded View).	115
Figure 7. 3 Small-Scale, Steel Plate LIFT Apparatus Test Assembly (Rear View). ...	115
Figure 7. 4: Small-Scale Steel Plate Test Arrangement.	116

Figure 7. 5: Steel Plate Nodes for Numerical Analysis of Conduction Heat Transfer.	119
Figure 7. 6: Thermal Conductivity of C-1018 Carbon Steel.	122
Figure 7. 7: Thermal Conductivity of Ceramic Fiber Insulation	123
Figure 7. 8: Thermal Conductivity of Air.	127
Figure 7. 9: Thermal Diffusivity of Air.....	127
Figure 7. 10: Kinematic Viscosity of Air.	128
Figure 7. 11: Specific Heat of C-1018 Carbon Steel.	130
Figure 7. 12: Temperature with Respect to Time – 7.2 kW/m ² Increased to 24.6 and 37.6 kW/m ²	133
Figure 7. 13: Measured and Calculated Heat Flux – 7.2 kW/m ² Increased to 24.6 and 37.6 kW/m ²	133
Figure 7. 14: Temperature with Respect to Time – 17.8 kW/m ² Increased to 43.0 kW/m ²	134
Figure 7. 15: Measured and Calculated Heat Flux – 17.8 kW/m ² Increased to 43.0 kW/m ²	134
Figure 7. 16: Temperature with Respect to Time – 28.8 kW/m ²	135
Figure 7. 17: Measured and Calculated Heat Flux – 28.8 kW/m ²	135
Figure 7. 18: Temperature with Respect to Time – 35.1 kW/m ² Increased to 47.8 kW/m ²	136
Figure 7. 19: Measured and Calculated Heat Flux – 35.1 kW/m ² Increased to 47.8 kW/m ²	136
Figure 7. 20: Temperature with Respect to Time – 36.7 kW/m ²	137
Figure 7. 21: Measured and Calculated Heat Flux – 36.7 kW/m ²	137
Figure 7. 22: Temperature with Respect to Time – 44.6 kW/m ²	138
Figure 7. 23: Measured and Calculated Heat Flux – 44.6 kW/m ²	138
Figure 7. 24: Temperature with Respect to Time – Medtherm Coating, 46.2 kW/m ² .	139
Figure 7. 25: Measured and Calculated Heat Flux – Medtherm Coating, 46.2 kW/m ²	139
Figure 8. 1: Typical Full-Scale Plate Thermocouple Attachment.	141
Figure 8. 2: Full Scale Test Steel Plate Assembly.	144
Figure 8. 3: Full-Scale Room/Corner Test Wall Heat Flux Measurement Configuration.	

.....	145
Figure 8. 4: Full-Scale Room/Corner Test Ceiling Heat Flux Measurement Configuration.	145
Figure 8. 5: Full-Scale Room/Corner Ceiling Test.....	147
Figure 8. 6: Room Gas Temperatures for 100 and 300 kW Energy Release Rates.....	156
Figure 8. 7: Example of the Added Incident Heat Flux from the Heated Room – 100 kW and 200 kW Burner.....	158
Figure 8. 8: Incident Heat Flux Distribution to the Walls and Ceiling from a 17 cm Square Corner Ignition Burner at 100 kW: Fire Plume Plus Cold Surface Correction Factor.	161
Figure 8. 9: Incident Heat Flux Distribution to the Walls and Ceiling from a 17 cm Square Corner Ignition Burner at 100 kW: Fire Plume Plus Heated Room Feedback and Cold Surface Correction Factor.....	162
Figure 8. 10: Incident Heat Flux Distribution to the Walls and Ceiling from a 17 cm Square Corner Ignition Burner at 300 kW: Fire Plume Plus Cold Surface Correction Factor.	163
Figure 8. 11: Incident Heat Flux Distribution to the Walls and Ceiling from a 17 cm Square Corner Ignition Burner at 100 kW: Fire Plume Plus Heated Room Feedback and Cold Surface Correction Factor.....	164
Figure 8. 12: Heat Flux Meter Measurements for 100, 200 and 300 kW Ignition Burner Energy Release Rates.	165
Figure 8. 13 (a & b): Heat Flux Distributions to the Wall from a 17 cm x 17 cm Propane Gas Burner Located in the Corner with Energy Release Rates of 100 and 300 kW [27].....	168
Figure 8. 14 (a & b): 100 kW and 300 kW Ignition Burner Flames.....	172
Figure 8. 15 (a & b): Flame Shape Generalizations for the 100 and 300 kW Burners Based on a Heat Flux Distribution Greater Than 30 kW/m ²	174

NOMENCLATURE

a	- upward flame spread acceleration parameter (long burnout time)
A	- surface area of sample
b	- upward flame spread acceleration parameter
c	- specific heat
d	- sample dimension
D	- burner dimension
g	- acceleration due to gravity (9.807 m/s^2)
Gr	- Grashof number
h_c	- convection heat transfer coefficient
ΔH_c	- effective heat of combustion
I	- flame intermittency
k	- thermal conductivity
k_{pc}	- thermal inertia
k_f	- flame length coefficient ($0.01 \text{ m}^2/\text{kW}$)
l	- length (length scale for h_c calculation)
l_m	- mean beam length
L	- effective heat of gasification
m	- mass
Nu	- Nusselt number
Pr	- Prandtl number
q	- heat transfer
Q	- energy
Ra	- Rayleigh number
t	- time
T	- temperature
U	- plume velocity
V	- flame spread velocity
z	- flame height in the Cone
Z	- flame height/length
α	- surface absorptivity
β	- volumetric thermal expansion coefficient
δ	- thickness, steel plate
Δ	- distance, between thermocouple nodes
ε	- emissivity
Φ	- lateral flame spread coefficient
κ	- absorption coefficient
ρ	- density
σ	- Stefan-Boltzmann constant ($5.670 \times 10^{-11} \text{ kW/m}^2 \cdot \text{K}^4$)
ν	- kinematic fluid viscosity

Subscripts

0	-	initial
a	-	air
b	-	burnout
c	-	convective
cold	-	incident to a cold surface
cr	-	critical
eff	-	effective
equil	-	equilibrium measurement
ext	-	external
f	-	flame or film (only in h_c calculation, Section 7)
fl	-	fluid
fo	-	flashover
h	-	horizontal, flame extension
hot	-	incident to a heated surface
i	-	incident
ig	-	ignition
inc	-	through the ceramic fiber insulation
init	-	initial measurement
k	-	conduction
meas	-	measured
min	-	minimum
net	-	net amount
p	-	pyrolysis
pl	-	plume
r	-	radiation
rr	-	re-radiation
R	-	room
s	-	surface
st	-	steel
sto	-	storage within the steel
v	-	vaporization or vertical portion of flame length (Section 8)
∞	-	ambient
peak	-	at the peak energy release rate
peak avg.	-	averaged over 80% above of the peak energy release rate
overall avg.	-	average of the overall properties during steady, sustained burning

Superscripts

(X'')	-	per unit area
(\dot{X})	-	per unit time
(\bar{X})	-	average value

1. INTRODUCTION

There are many different aspects of a fire event that can affect the final outcome. One means of expressing the overall hazard associated with a particular fire scenario is in terms of the size of the fire. The primary mechanism by which fires grow from a small incipient fire to a large, possibly fully involved, one is through the ignition and flame spread across the various fuels that are available. When attempting to determine or predict the growth rate potential and overall fire size for a space, the flame spread over the furnishings and interior finish materials will become significant. The fire growth of a fire can be considered to be a critical event in which the outcome can be based on several parameters. One method for determining the fire growth potential of interior finish materials is by the room-corner test. Unlike most other tests, materials in the room-corner test are exposed to a full-scale fire scenario: the materials are mounted in an orientation that is representative of their use in real situations and the ignition source is more consistent with realistic forms of ignition.

1.1 Room-Corner Tests

Several room-corner test protocols are currently in use and are listed by the American Society of Testing and Materials (ASTM), the National Fire Protection Association (NFPA), the Uniform Building Code (UBC) and the International Standards Organization (ISO). The tests arrangements and procedures are all similar, but have some differences that can significantly affect the performance of the sample material. These differences include the size, location and energy release rate of the ignition burner as well as the sample mounting.

The test method addressed in this analysis is the ISO 9705 Full-Scale Room Fire Test for Surface Products [22] or more simply the Room-Corner Test. The choice of this method was motivated by the fact that the ISO 9705 test is an internationally recognized standard and the availability of test data and a full-scale test facility.

The ISO 9705 test has the following criteria and can be seen in Figure 1.1:

- Room: 2.4 m x 3.6 m x 2.4 m high.
- Door on Short Wall: 2.0 m x 0.8 m wide.
- Ignition Burner: 17 cm x 17 cm square sand burner, top surface 30 cm above the floor, propane fuel.
- Burner Location: Corner, in contact with both walls.
- Burner Output: 100 kW for 10 minutes followed by 300 kW for an additional 10 minutes.
- Material Mounting: On the 3 walls opposite the doorway and on the ceiling if desired.

One useful way of ranking materials and determining the fire growth potential for a particular material is by the time to flashover under the conditions specified by the test standard. Flashover is an altogether complex process and is associated with different characteristics of the fire compartment: heat flux to the floor of approximately 20 kW/m^2 , an upper layer temperature of 500 to 600 °C and flames emerging from the doorway [11]. Based on the standard room geometry of the test method, flashover conditions typically coincide with an

energy release rate of about 1,000 kW. It must be recognized that the presence or absence of the sample material on the ceiling of the room can be one of the most significant factors as to whether or not flashover occurs.

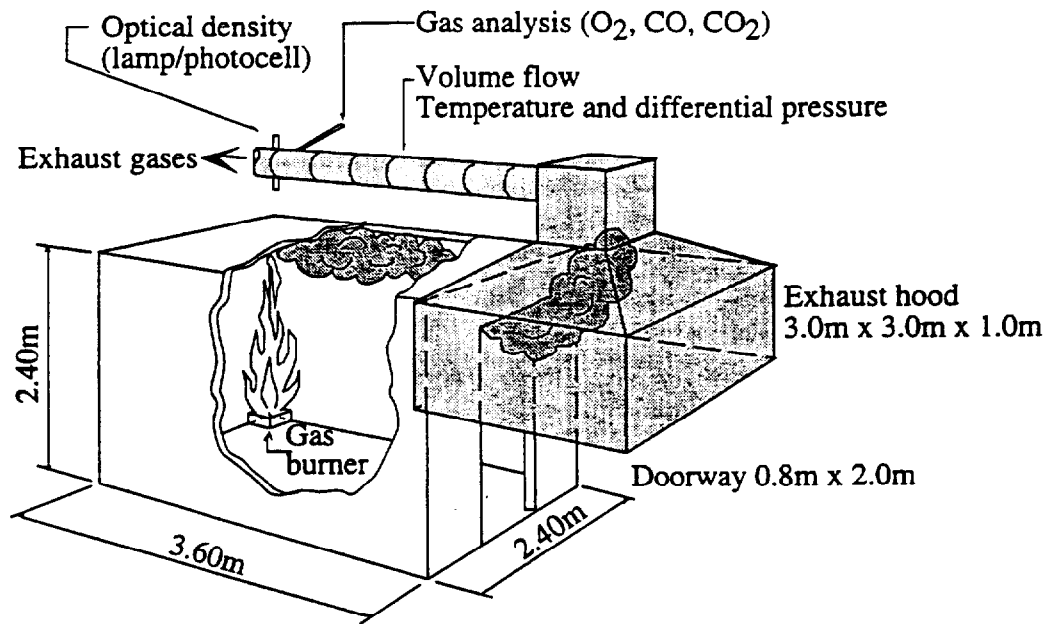


Figure 1. 1: Schematic Drawing of the ISO 9705 Room-Corner Test [49].

1.2 Modeling

A mathematical model to predict the fire growth of materials in a room-corner test has been developed by Quintiere [36]. The model utilizes derived material fire properties and simple equations that govern the physics of ignition and flame spread to predict the time dependent area of burning, upper gas layer temperature and energy release rate for a material in the room-corner test.

A primary difference between the different room-corner test methods is the ignition source. Test results indicate that the energy release rate of the burner, the associated heat flux to the sample material and the duration of the exposure influence the performance of the material. This is particularly true for thin materials and materials with a short burning duration. By adjusting the exposure conditions and material fire properties, the model can be used to indicate how sensitive a material is to producing flashover conditions. The model allows the performance of materials with different ignition sources and room geometries to be predicted without performing many expensive full-scale experiments. The model can also be adapted to wall fires and open pool fires, but will be confined to the prescriptions of the ISO standard for this analysis.

The materials evaluated represent traditional materials as well as materials that could be a potential challenge to the model. Previous analyses [23, 36, 37] have shown that charring materials like wood are typically well predicted by the model. However, thermoplastic materials can melt, deform and drip from the wall and ceiling which presents a significant modeling complexity. The series of materials evaluated in this analysis represent a wide range of realistic materials which should indicate the strengths and weaknesses of the model.

In order to analyze the performance of the materials, a systematic method will be developed for determining the material fire properties required by the model. This method will be based on small-scale test results like the Cone Calorimeter [2] and the LIFT [1] and medium-scale test methods like Roland [51]. Although the procedure for deriving the properties is not perfect for every material, it will be applied to each

material as a first step in developing a uniform system. Specific areas where the method breaks down will be indicated, analyzed, and explained.

Due to the critical nature of some materials, an empirical correlation by Cleary and Quintiere [9] will be applied to the materials. Using the same material properties used for modeling along with information regarding the ignition source, the flashover potential for the materials will be determined and presented in a format that allows materials to be compared.

Several aspects of the current model can be improved. Various studies have been conducted in order to examine the heat flux from controlled fires to vertical walls and corners [7, 23, 26, 31, 52, 53]. This heat flux information has been found to be very important to the performance of materials in the room-corner scenario and more generally for wall flame spread. More detailed experiments are needed in this area, especially for the exposure of materials in accordance with the standard test methods. It is recognized that theoretical determinations of these heat fluxes is beyond the current state of the art and experimentally based correlations will have to be utilized.

The incident heat flux to materials in the room-corner test is approximated in the model. In order to better understand the actual exposure conditions, full-scale heat flux measurements have been made and detailed heat flux profiles have been created as a part of this research. In addition, flame heights for the ignition burner in the corner have been determined. These factors will provide a tremendous amount of knowledge to what is currently known about the room-corner test and will enable Quintiere's model to be improved.

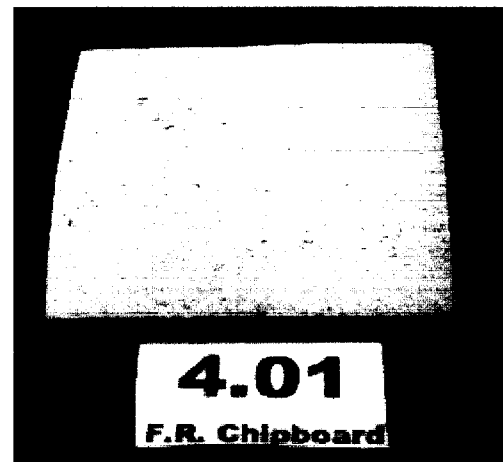
In response to the need for improved performance predictions, this research will attempt to provide a systematic method for determining material fire properties, assess the accuracy of a fire growth model for the room-corner test and determine aspects of the standard test that can be used to improve the current model.

2. DESCRIPTION OF MATERIALS

Thirteen materials were provided to the University of Maryland, for prediction of their performance in the full-scale room-corner test using Quintiere's fire growth model [36]. These materials are the same as the ones tested in the Cone Calorimeter [1] and Roland apparatus [51] at the L. S. Fire Laboratories (LSF), Moutano, Italy. Each material was tested in the Cone five times at four different external heat flux levels—25, 35, 40 and 50 kW/m²—for a total of twenty tests for each material. These same materials were also tested using the ISO 9705 Room-Corner test protocol at the Swedish National Testing and Research Institute, Boras, Sweden [49]. These materials are listed below—the number preceding each material refers to the LSF designation for each material and will be used interchangeably with the full name. A brief description of the material properties and the manner in which the samples were mounted for the full-scale room-corner test are provided. All of the materials were conditioned at 20 ± 5 °C prior to the full-scale tests. Photographs of the samples are also provided.

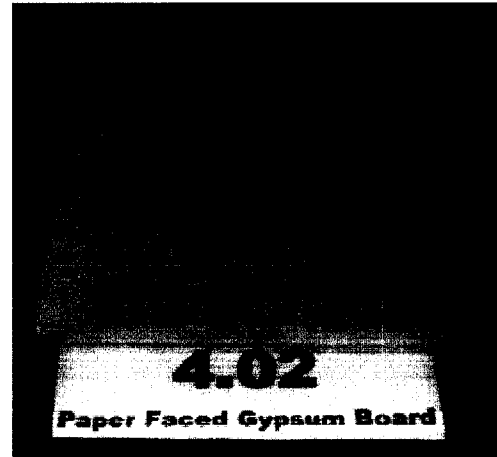
R 4.01 Fire Retarded Chipboard

- Thickness: 12 mm
- Density: 805 kg/m³
- Moisture content: 6.8 %
- Mounting: Nailed to the light weight concrete walls and ceiling.



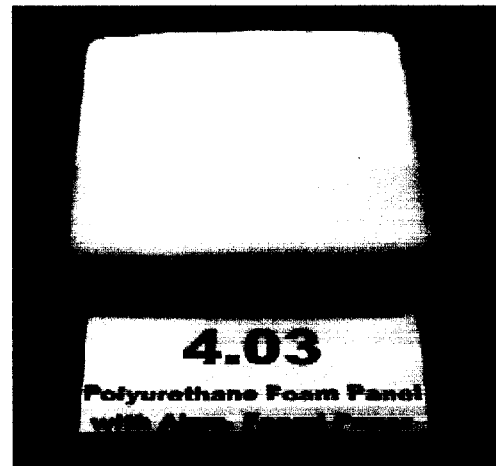
R 4.02 Paper Faced Gypsum Wallboard

- Thickness: 12.5 mm
- Density: 720 kg/m³
- Mounting: Nailed to the light weight concrete walls and ceiling.



R 4.03 Polyurethane Foam Panel with Aluminum Paper Facing

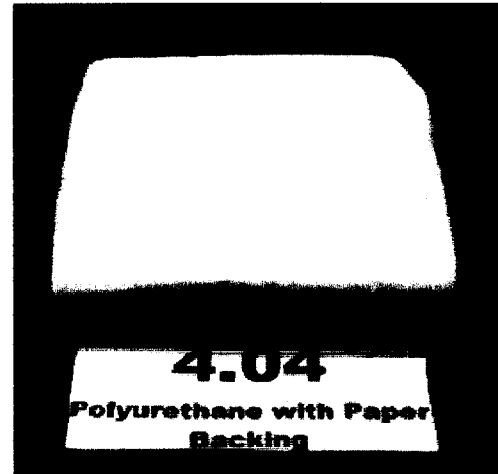
- Thickness: 41 mm
- Density: 38 kg/m³
- Area weight: 2.03 kg/m²
- Mounting: Glued to a non-combustible board called "Promatek H", density 870 kg/m³, with a water based contact adhesive called "Casco 3880".



The non-combustible boards were nailed to the light weight concrete walls and ceiling before the polyurethane foam panels were glued.

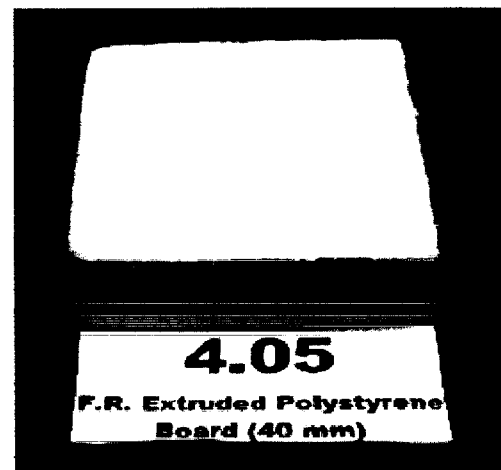
R 4.04 Polyurethane Foam Panel with Paper Facing

- Thickness: 40 mm
- Density: 38 kg/m³
- The properties for this material were used to predict the performance of the polyurethane foam panel with aluminum facing, R 4.03, due to the problems encountered in extrapolating adequate material properties (see Section 3).



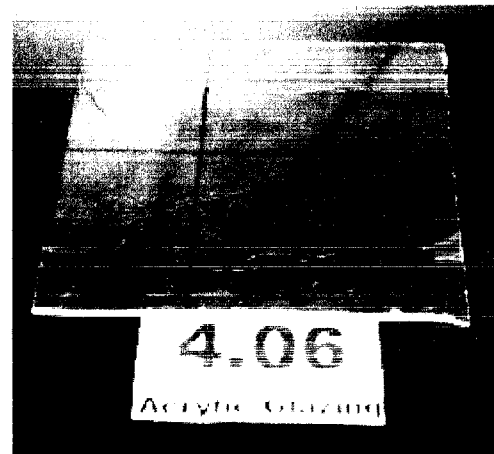
R 4.05 Fire Retarded, Extruded Polystyrene Board (40 mm)

- Thickness: 40 mm
- Density: 33 kg/m³
- Mounting: Glued to a non-combustible board called "Promatek H", density 870 kg/m³, with a water based contact adhesive called "Casco 3880". The non-combustible boards were nailed to the light weight concrete walls and ceiling before the polystyrene boards were glued.



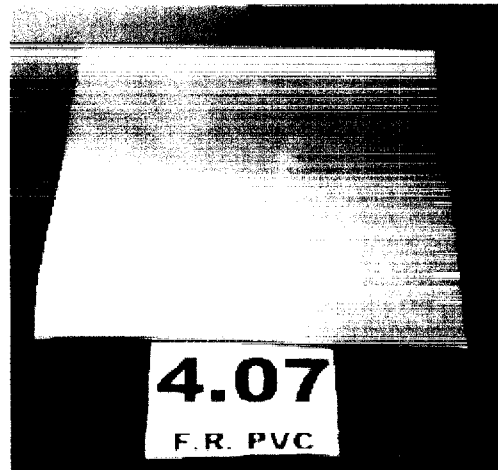
R 4.06 Clear Acrylic Glazing

- Thickness: 3 mm
- Density: 1150 kg/m³
- Mounting: Screwed to a frame of light steel profiles spaced 40 mm from the light weight concrete walls and ceiling.



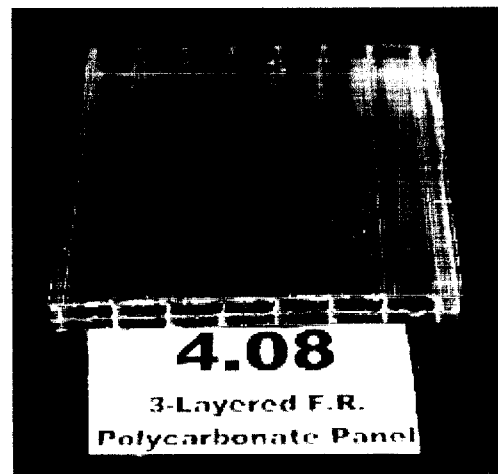
R 4.07 Fire Retarded PVC

- Thickness: 3 mm
- Density: 1505 kg/m³
- Mounting: Screwed to a frame of light steel profiles spaced 40 mm from the concrete walls and ceiling.



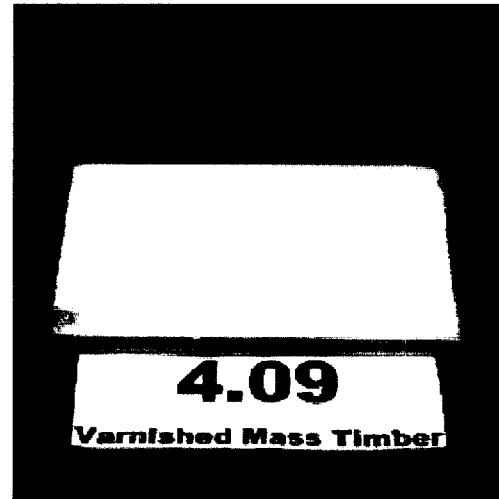
R 4.08 3-Layered Clear, Fire Retarded Polycarbonate Panel

- Thickness: 16 mm
- Density: 1200 kg/m³
- Area weight: 2.9 kg/m²
- Mounting: Screwed to a frame of light steel profiles spaced 40 mm from the light weight concrete walls and ceiling.



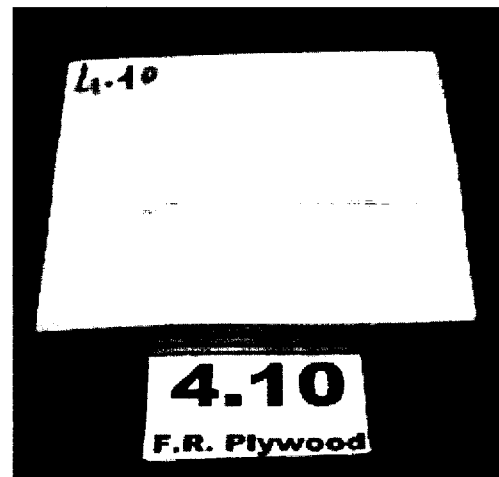
R 4.09 Varnished Massive Timber Paneling

- Thickness: 9 mm
- Area weight: 3.4 kg/m²
- Moisture content: 9.6 %
- Mounting: Nailed to the light weight concrete walls and ceiling.



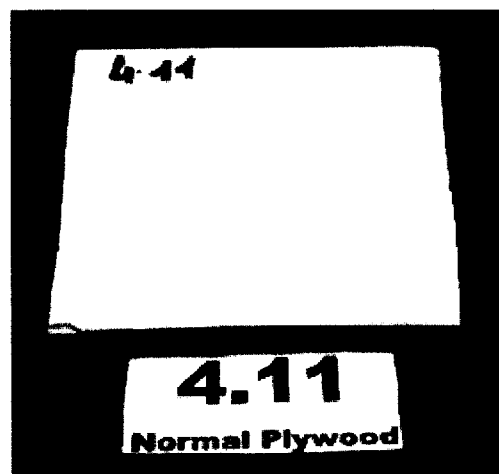
R 4.10 Fire Retarded Plywood

- Thickness: 15 mm
- Density: 460 kg/m³
- Moisture content: 9.8 %
- Mounting: Nailed to the light weight concrete walls and ceiling.



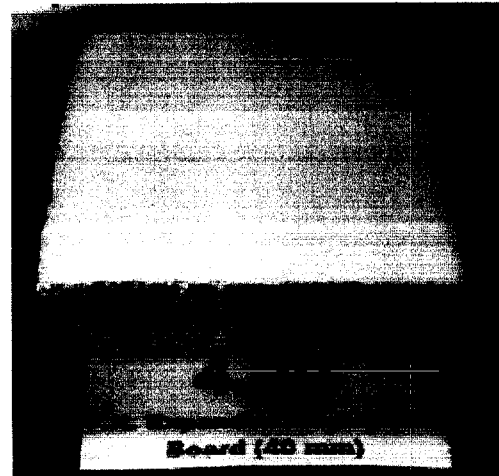
R 4.11 Normal, Untreated Plywood

- Thickness: 15 mm .
- Density: 440 kg/m³
- Moisture Content: 11.3 %
- Mounting: Plywood was nailed to the light weight concrete walls and ceiling.



R 4.20 Fire Retarded, Expanded Polystyrene Board (40 mm)

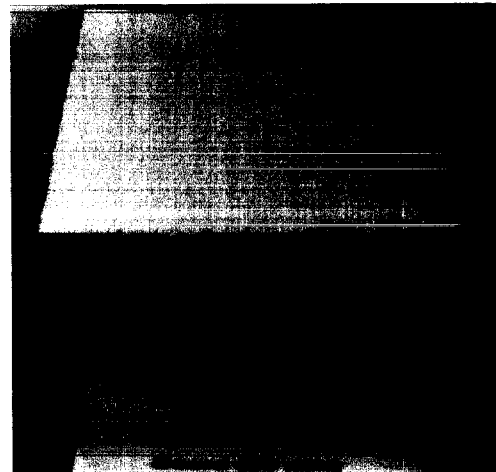
- Thickness: 40 mm
- Density: 30 kg/m³
- Mounting: Glued to a non-combustible board called “Promatek H”, density 870 kg/m³, with a water based contact adhesive called “Casco 3880”. The non-combustible boards were nailed to the light weight



concrete walls and ceiling before the polystyrene boards were glued.

R 4.21 Fire Retarded, Expanded Polystyrene Board (80 mm)

- Thickness: 80 mm
- Density: 17 kg/m³
- Mounting: Glued to a non-combustible board called “Promatek H”, density 870 kg/m³, with a water based contact adhesive called “Casco 3880”. The non combustible boards were nailed to the light weight



concrete walls and ceiling before the polystyrene boards were glued.

3. DETERMINING MATERIAL PROPERTIES

The material properties required to run the fire growth model are typically derived from data provided by the Cone Calorimeter (ASTM E-1354 [2], ISO 5660) and the Lateral Ignition and Flame Spread Test (LIFT, ASTM E-1321 [1], ISO 5658). However, for this analysis the flame spread data was provided by the Roland apparatus instead of the LIFT [46]. These modeling properties are listed in Table 3.1.

Table 3. 1: Material Modeling Properties.

Material Property	Symbol	Test Method
1. Ignition Temperature	T_{ig}	Cone, LIFT or Roland
2. Minimum Temperature for Lateral Flame Spread	$T_{s, min}$	LIFT or Roland
3. Thermal Inertia	$k\rho c$	Cone or LIFT
4. Lateral Flame Spread Parameter	Φ	LIFT or Roland
5. Effective Heat of Combustion	ΔH_C	Cone
6. Effective Heat of Gasification	L	Cone
7. Total Energy per Unit Area	Q''	Cone

Previous analyses of the performance of materials have used inconsistent methods for determining the material properties. Therefore a more systematic method for accurately determining these properties will be developed. This systematic method will then be applied to all of the materials and used to predict the performance in the full-scale room/corner test.

3.1 Ignition Properties

The ignition properties for the LSF materials were determined by Dillon, Kim and Quintiere [10] based on the Cone Calorimeter test results. In general the time to ignition (t_{ig}) can be expressed as

$$t_{ig} = C \cdot k\rho c \frac{(T_{ig} - T_{\infty})^2}{(\dot{q}_i'' - \dot{q}_{cr}'')^2} \quad (3.1)$$

where T_{∞} is the ambient temperature (K), \dot{q}_i'' is the incident radiant heat flux (kW/m²), \dot{q}_{cr}'' is the critical heat flux for ignition (kW/m²) and C depends on \dot{q}_i'' . For the analysis by Dillon *et al.*, C was taken to be $\pi/4$ for high incident heat flux values. The critical heat flux for ignition can be expressed as

$$\dot{q}_{cr}'' = \sigma(T_{ig}^4 - T_{\infty}^4) + h_c(T_{ig} - T_{\infty}) \quad (3.2)$$

where σ is the Stefan-Boltzmann constant (5.670×10^{-11} kW/m²·K⁴) and h_c is the convective heat transfer coefficient (kW/m²·K).

A plot of the inverse square root of the ignition times ($t_{ig}^{-1/2}$) with respect to the incident heat flux from the Cone is used to determine T_{ig} and $k\rho c$ (see Figure 3.1). The critical heat flux is the point at which t_{ig} is infinite and therefore $t_{ig}^{-1/2}$ is equal to 0. A value for \dot{q}_{cr}'' is determined by extrapolating the data at low heat fluxes as shown in Figure 3.1. The critical heat flux for each material is presented in Table 3.2. Using an h_c value of 10 kW/m²·K for the Cone, the critical heat flux is used in Equation 3.2 to calculate T_{ig} . The slope of the linear fit through the data points equals

$$\frac{1}{\left(\frac{\pi}{4} \cdot k\rho c\right)^{1/2} (T_{ig} - T_{\infty})}$$

and is used to calculate $k\rho c$. The ignition data figures for all of the LSF materials are presented by Dillon *et al.*

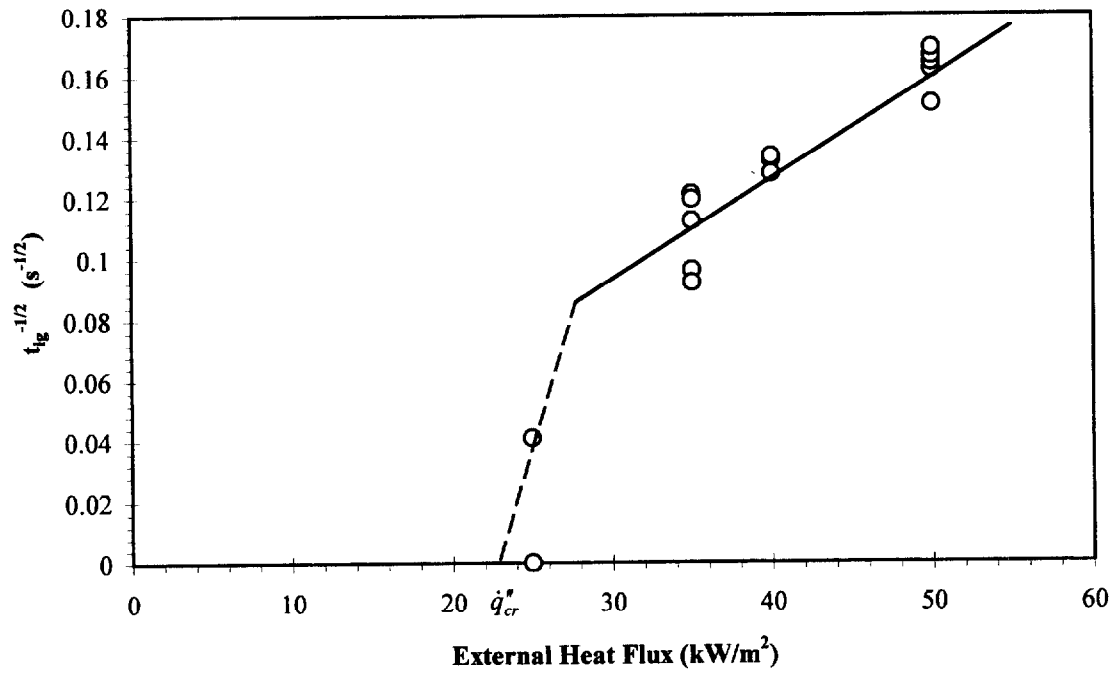


Figure 3. 1: Typical Interpretive Plot of Ignition Data in Order to Derive Properties: R 4.21, Fire Retarded Expanded Polystyrene Board.

Table 3. 2: Estimated Critical Heat Flux for Ignition

Material	\dot{q}_{cr}''
R 4.01, FR. Chipboard	25
R 4.02, Gypsum	26
R 4.03, PU/Alum. *	----
R 4.04, PU/Paper	6
R 4.05, Ext. PS40	7
R 4.06, Acrylic	4
R 4.07, FR. PVC	16
R 4.08, 3-Layer PC	24
R 4.09, Mass Timber	10
R 4.10, FR. Plywood	22
R 4.11, Plywood	8
R 4.20, Exp. PS40	8
R 4.21, Exp. PS80	23

3.2 Flame Spread Properties

The flame spread data for the LSF materials were also determined by Dillon *et al.* [10] and were obtained by using the Roland apparatus instead of the LIFT. A typical flame spread test using the Roland apparatus can be seen in Figure 3.2. The Equation for the flame spread velocity, V , is

$$V = \frac{\Phi}{k\rho c(T_{ig} - T_s)^2} \quad (3.3)$$

where Φ is the lateral flame spread parameter (kW^2/m^3) and T_s the surface temperature of the material caused by the incident heat flux (K). The location on the surface of the material at which lateral flame spread ceases can be used to determine $T_{s, min}$. The lateral flame spread parameter can then be calculated using Equation 3.3.

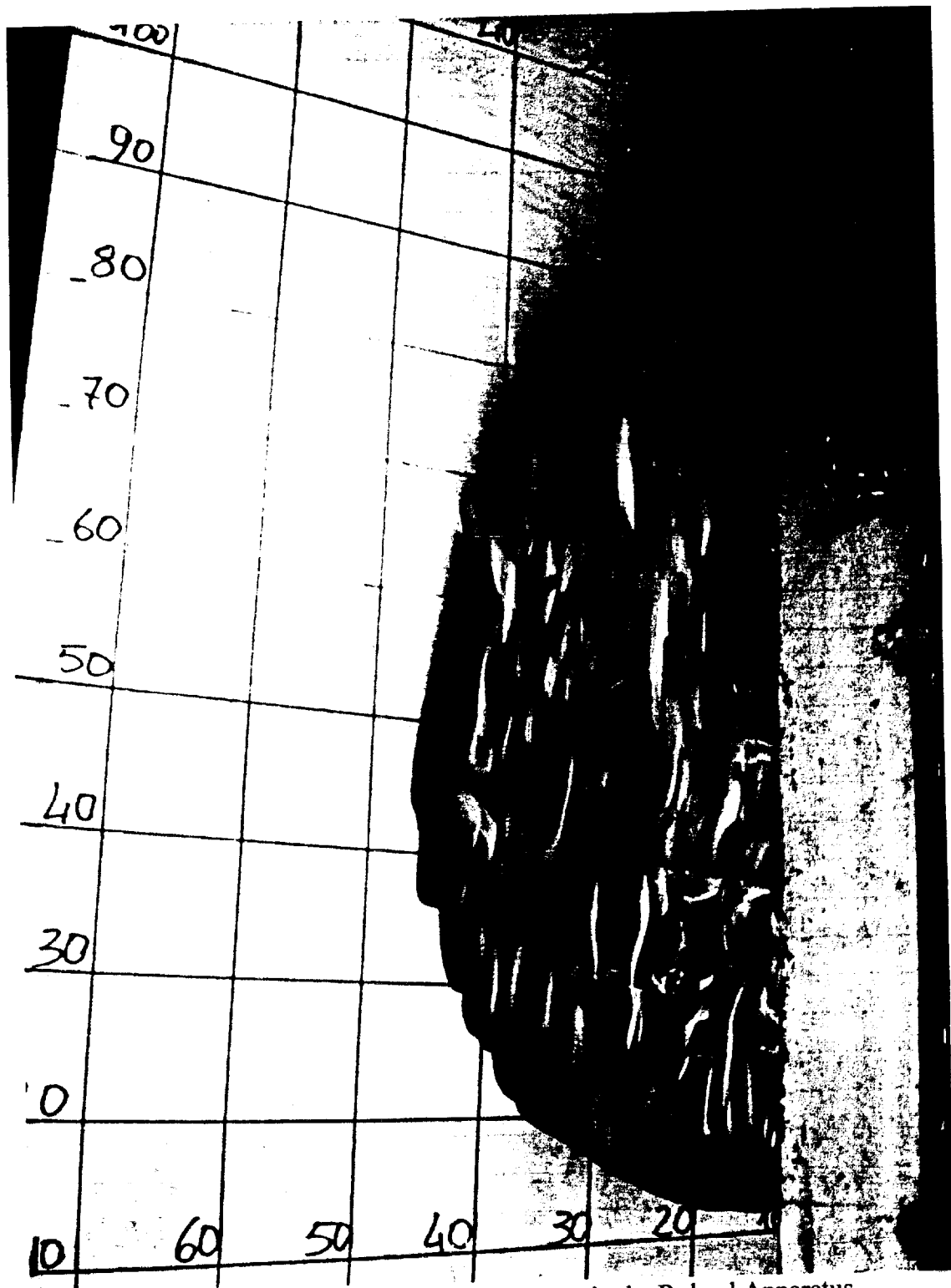


Figure 3. 2: A Typical Burning Process in the Roland Apparatus

The ignition and flame spread properties were derived by the methods presented in Sections 3.1 and 3.2 and are presented in Table 3.3.

Table 3. 3: Ignition and Flame Spread Properties of the LSF Materials.

Material	T_{ig} (°C)	$T_{s,min}$ (°C)	$k\rho c$ [(kW/m ² K) ² s]	Φ (kW ² /m ³)
R 4.01, FR. Chipboard	505	507	4.024	0.0
R 4.02, Gypsum	515	517	0.549	0.0
R 4.03, PU/Alum.*	---	---	---	0.0
R 4.04, PU/Paper	250	77	0.199	8.7
R 4.05, Ext. PS40	275	77	1.983	1.2
R 4.06, Acrylic	195	195	2.957	---
R 4.07, FR. PVC	415	352	1.306	0.2
R 4.08, 3-Layer PC	495	167	1.472	0.0
R 4.09, Mass Timber	330	77	0.530	6.9
R 4.10, FR. Plywood	480	197	0.105	0.7
R 4.11, Plywood	290	147	0.633	2.2
R 4.20, Exp. PS40	295	77	1.594	4.2
R 4.21, Exp. PS80	490	77	0.557	7.1

* Material properties could not be extrapolated from the test data

3.3 Heat of Combustion (ΔH_C)

3.3.1 Definition

The enthalpy of combustion or heat of combustion (ΔH_C) is a constant material property, representing the total amount of energy released by a unit mass of fuel (kJ/g) when it is completely oxidized through the combustion process. Heat of combustion values can be determined using an oxygen bomb calorimeter which forces all of the material to combust in a pure oxygen atmosphere while the vessel temperature and specimen mass loss are carefully monitored. Heat losses from the system are

minimized so that the heat release can be accurately determined by the temperature rise. The gross heat of combustion, $\Delta H_{C, gross}$, can then be calculated by dividing the total heat release by the total specimen mass loss. Gross heat of combustion values for many materials are presented by Tewarson [47]. However, complex materials like wood and composites like gypsum wallboard burning in more realistic conditions will not exhibit the gross heat of combustion values obtained in the oxygen bomb. Char formation, moisture evaporation and other complex effects will cause a reduced $\Delta H_{C, gross}$ to be observed. Therefore an effective heat of combustion, $\Delta H_{C, eff}$, which better represents the material burning in actual conditions needs to be determined. This effective value (simply referred to as ΔH_C for convenience) can be used to determine the energy release rate per unit area from a material based on the mass loss rate by:

$$\dot{Q}'' = \Delta H_C \cdot \dot{m}'' \quad (3.4)$$

where \dot{Q}'' is the energy release rate per unit area (kW/m²) and \dot{m}'' is the mass loss rate per unit area (g/s·m²). In this definition of the effective heat of combustion, \dot{m}'' of a burning material may not represent the mass of the fuel alone and can represent a loss of moisture or other products. This can result in complications in the determination of suitable values for predicting performance.

3.3.2 Determining ΔH_C

The time-varying and average effective heat of combustion were measured by LSF using the Cone Calorimeter. Each material was tested five times at each of the following incident heat flux levels: 25, 35, 40 and 50 kW/m². The Cone Calorimeter standard [2] specifies the time-varying heat of combustion value to be calculated by

$$\Delta H_c(t) = \frac{\dot{Q}''(t)}{\dot{m}''(t)}$$

where $\dot{Q}''(t)$ and $\dot{m}''(t)$ are the energy release rate and mass loss rate per unit area at time t . Similarly, the average heat of combustion is calculated by

$$\Delta H_c = \frac{Q}{\Delta m} \quad (3.5)$$

where Q is the total energy released during the test and Δm is the total specimen mass loss.

Because ΔH_c is typically considered to be a constant material property, it should not vary with temperature, burning rate or incident heat flux. Nevertheless, the Cone data indicates that the measured heat of combustion values were not constant with respect to time, and in some cases varied significantly throughout the test (see Figure 3.3). These fluctuations are most likely due to complex burning effects and inaccuracies in the oxygen consumption calorimetry method used to determine the values. Therefore three different methods will be utilized for determining constant effective heat of combustion values from the Cone Calorimeter data: based on (1) the peak energy release rate, (2) an average energy release rate around the peak and (3) the overall energy released during the test. Examples of these three energy release rates are presented in Figure 3.4.

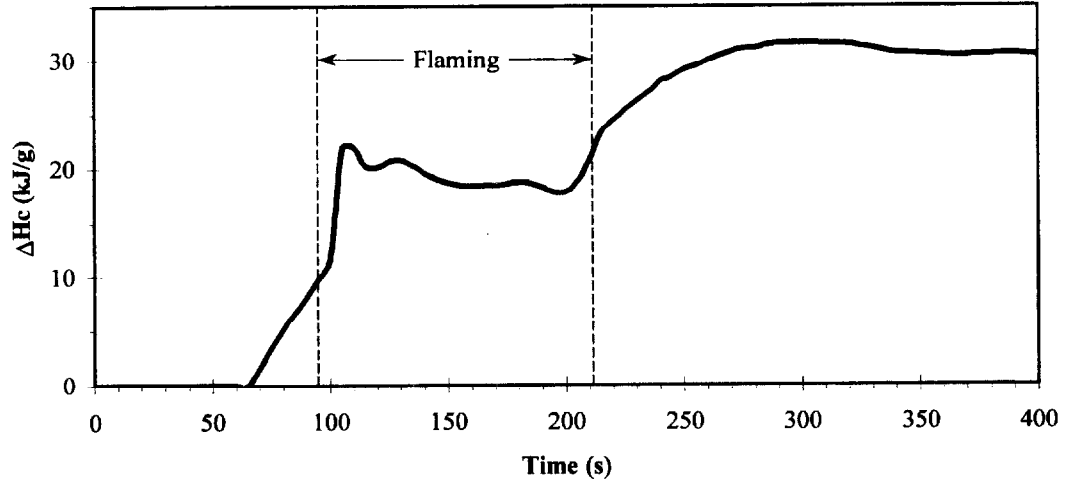


Figure 3. 3: Example of Time-Varying Heat of Combustion Measured in the Cone Calorimeter: R 4.08, 3-Layer Polycarbonate Panel at 50 kW/m² in the Cone Calorimeter.

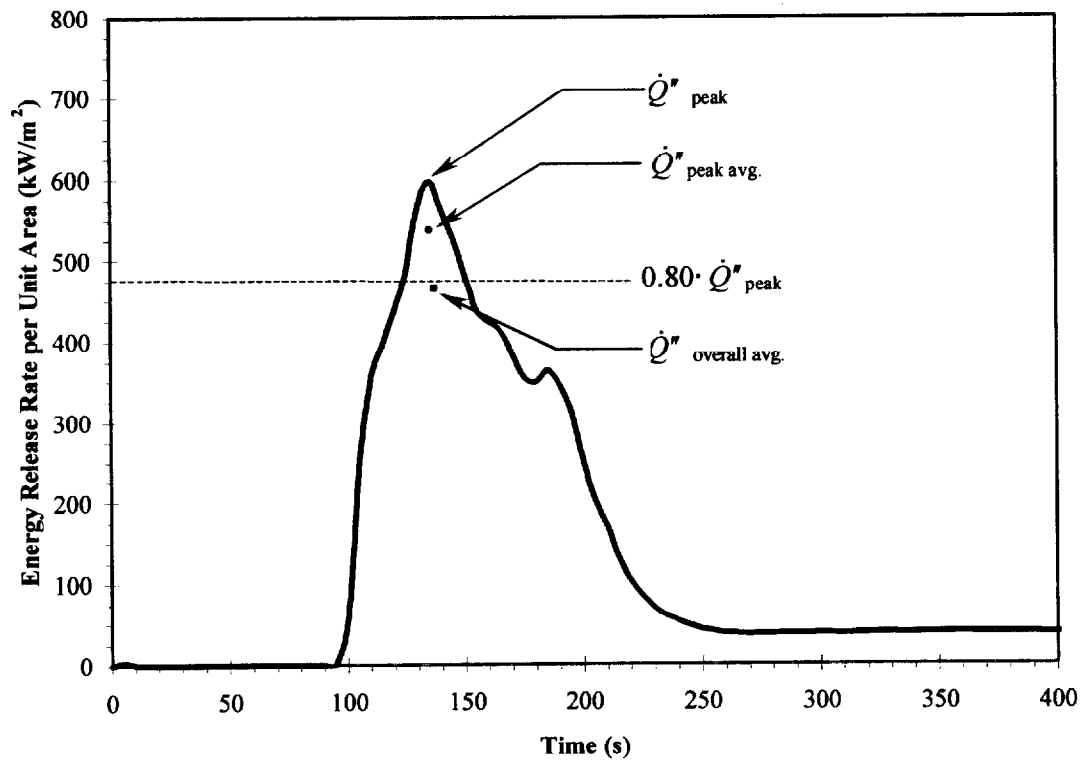


Figure 3. 4: Example of Peak, Peak Average and Overall Average Energy Release Rates per Unit Area Measured in the Cone Calorimeter: R 4.08 at 50 kW/m² in the Cone.

Due to the fact that not all of the samples ignited or exhibited continuous flaming, only the test data associated with ignition and sustained burning were used to determine the effective ΔH_C values. In a few tests the LSF data reports ignition of a sample, but inspection of the energy release rate versus time graphs clearly indicated that actual sustained flaming did not occur. Data from these types of tests will be omitted from the determination of the heat of combustion values.

Examples of $\Delta H_{C, peak}$, $\Delta H_{C, peak avg.}$ and $\Delta H_{C, overall avg.}$ values are shown graphically in Figure 3.5 and the three effective values for each material are presented in Table 3.4. Theoretically all three of these values should be identical, and as the table indicates there is reasonably good agreement between the values. The three methods for determining ΔH_C are explained below.

3.3.2.1 Peak Rate of Energy Release ($\Delta H_{C, peak}$)

For each Cone test in which the material ignited, a peak or maximum rate of energy release (\dot{Q}''_{peak}) occurs (see Figure 3.4). A heat of combustion value can be determined which directly coincides with the time at which the peak energy release rate occurs (see Figure 3.5). This “peak” value does not represent the maximum heat of combustion that was measured, but in fact represents the heat of combustion value associated with the peak energy releases rate.

All of the “peak” heat of combustion values measured for a particular material can then be averaged to determine an average, $\overline{\Delta H_{C, peak}}$, value. When plotted with respect to the external heat flux, the average value represents a horizontal “best-fit” line through the peak value data which can be seen in Figure 3.6. Figures for all of the

materials are presented by Dillon *et al.* [10]. These average heat of combustion values are listed in Table 3.4. This average peak heat of combustion value can be used in Equation 3.4 to determine the typical peak energy release rate associated with a material.

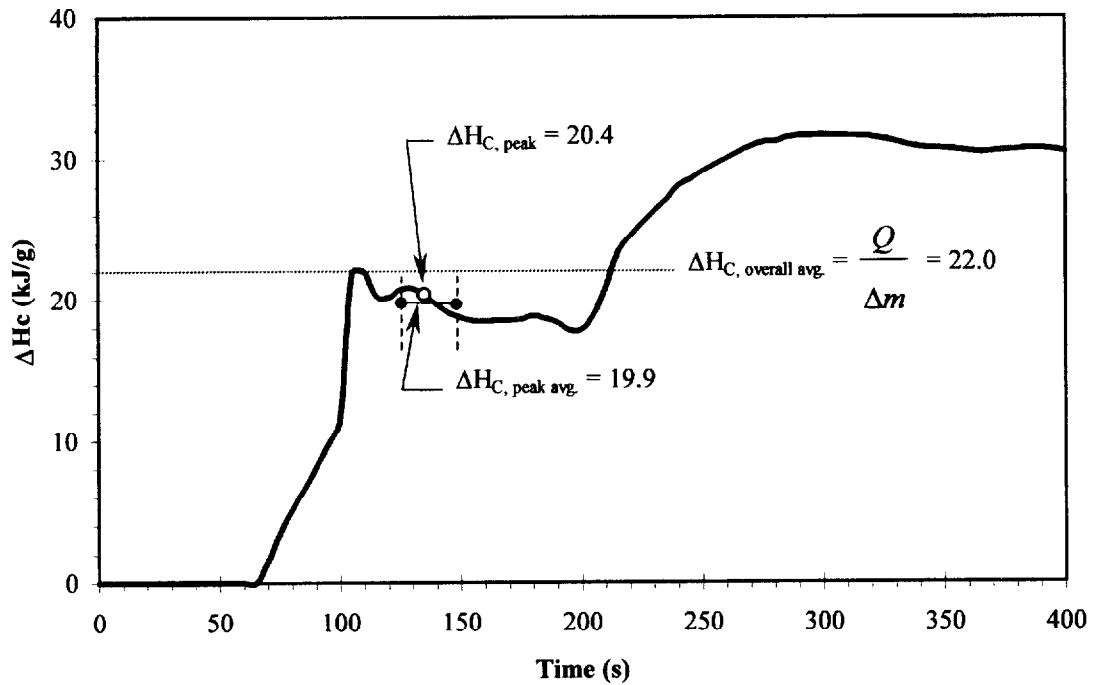


Figure 3. 5: Method of Determining the Peak, Peak Average and Overall Average Heat of Combustion Values: R 4.08, 3-Layer Polycarbonate Panel at 50 kW/m² in the Cone Calorimeter.

3.3.2.2 Average Rate of Energy Release ($\Delta H_{c, \text{peak avg.}}$)

Another method of using the peak energy release rate as a basis for determining the effective heat of combustion is to take an average energy release rate per unit area around the peak value. For this analysis, it is estimated that an average peak energy

release rate occurs approximately 20% below the peak value. Therefore, the $\dot{Q}''_{\text{peak avg}}$ shown in Figure 3.4 is an integrated average of the measured energy release rates above 80% of the peak value. The “peak average” value is intended to represent an energy release rate that is more consistent with steady burning as opposed to an instantaneous maximum value. This averaging method reduces the effects of a sudden, possibly uncharacteristic spike in the energy release rate and smoothes the data while still taking into account the most intense burning of the material.

The peak average heat of combustion, $\Delta H_{C, \text{peak avg.}}$, is taken to be a numerical average of the measured heat of combustion values over the same time interval that the energy release rate is averaged. The time period over which the heat of combustion values are averaged is illustrated in Figure 3.5. An average value, $\overline{\Delta H_{C, \text{peak avg.}}}$, is calculated to be a numerical average of the individual peak average values from each test.

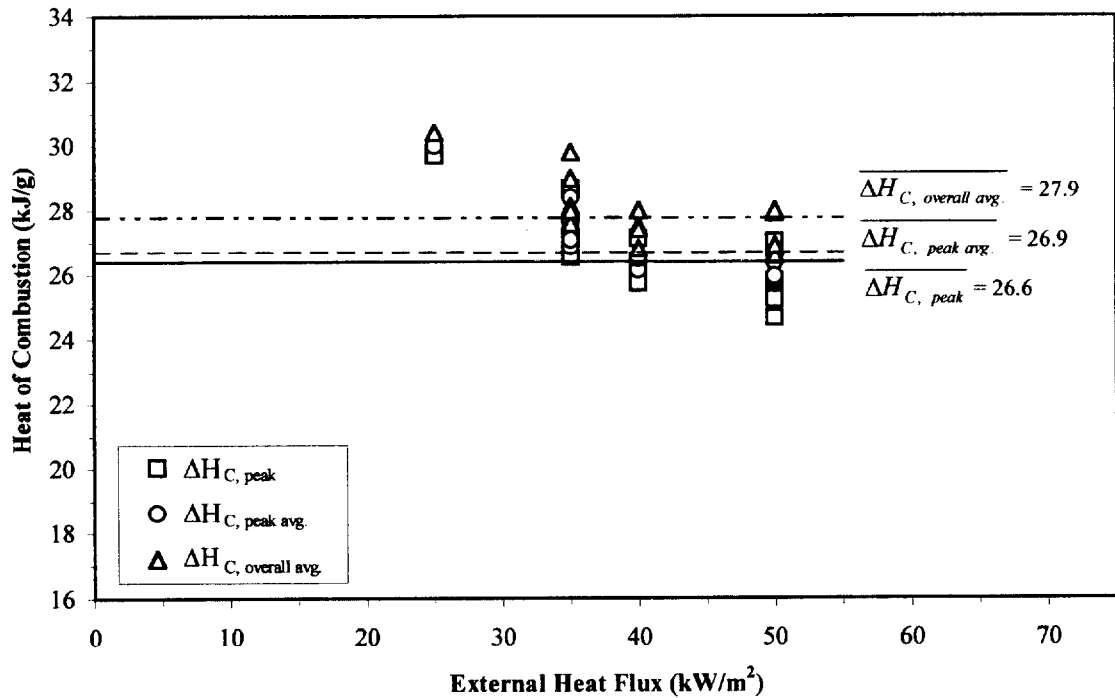


Table 3. 4: Average, Effective Heat of Combustion (ΔH_c) Values Calculated by Three Methods.

Material	$\overline{\Delta H_{C, peak}}$ (kJ/g)	$\overline{\Delta H_{C, peak avg.}}$ (kJ/g)	$\overline{\Delta H_{C, overall avg.}}$ (kJ/g)
R 4.01, FR. Chipboard	9.6	9.2	7.9
R 4.02, Gypsum	6.7	6.4	3.2
R 4.03, PU/Alum.	16.3	16.3	18.2
R 4.04, PU/Paper	19.3	18.9	18.0
R 4.05, Ext. PS40	28.5	27.8	28.2
R 4.06, Acrylic	24.2	24.1	24.0
R 4.07, FR. PVC	10.2	9.9	6.8
R 4.08, 3-Layer PC	19.5	19.5	21.5
R 4.09, Mass Timber	17.3	16.3	15.7
R 4.10, FR. Plywood	11.6	11.2	10.3
R 4.11, Plywood	12.1	11.9	10.8
R 4.20, Exp. PS40	27.4	27.5	27.8
R 4.21, Exp. PS80	26.6	26.9	27.9

3.4 Heat of Gasification (L)

3.4.1 Definition

When exposed to an incident heat flux, materials will vaporize at a certain rate. The rate of this vaporization can be expressed in terms of the mass loss rate per unit area of material (\dot{m}'') and is dependent on the magnitude of the heat flux. The heat of gasification (L) value is an effective property that describes the energy required to produce the fuel volatiles per unit mass of the material and is typically expressed in the units kJ/g. The effective L value represents the average effects of vaporization of the fuel and does not include transient burning effects. Typical heat of gasification values have been determined by Tewarson [47].

The burning of a material is a relatively complex and unsteady process. However, a constant, steady burning rate per unit area can be approximated using constant net heat flux and heat of gasification values:

$$\dot{m}'' = \frac{\dot{q}''_{net}}{L} \quad (3.6)$$

where \dot{q}''_{net} is the net heat flux to the material (kW/m²). This approximation assumes that at ignition (t_{ig}) the burning rate becomes \dot{q}''_{net}/L and at the burnout time (t_b) it drops to zero. This burning rate approximation is illustrated in Figure 3.7, where the area under the predicted curve is equivalent to the area under the experimental curve. The predicted ignition time in the figure is approximated using the following expression:

$$t_{ig} = \frac{\pi}{4} \cdot k\rho c \frac{(T_{ig} - T_{\infty})^2}{(\dot{q}''_{net})^2}$$

and the burnout time is approximated by

$$t_b = \frac{L}{\Delta H_c} \frac{Q''}{\dot{q}''_{net}}$$

where Q'' is the total energy per square meter of material (see Section 3.5). Therefore in order to estimate the steady burning rate of materials, an effective heat of gasification value needs to be determined.

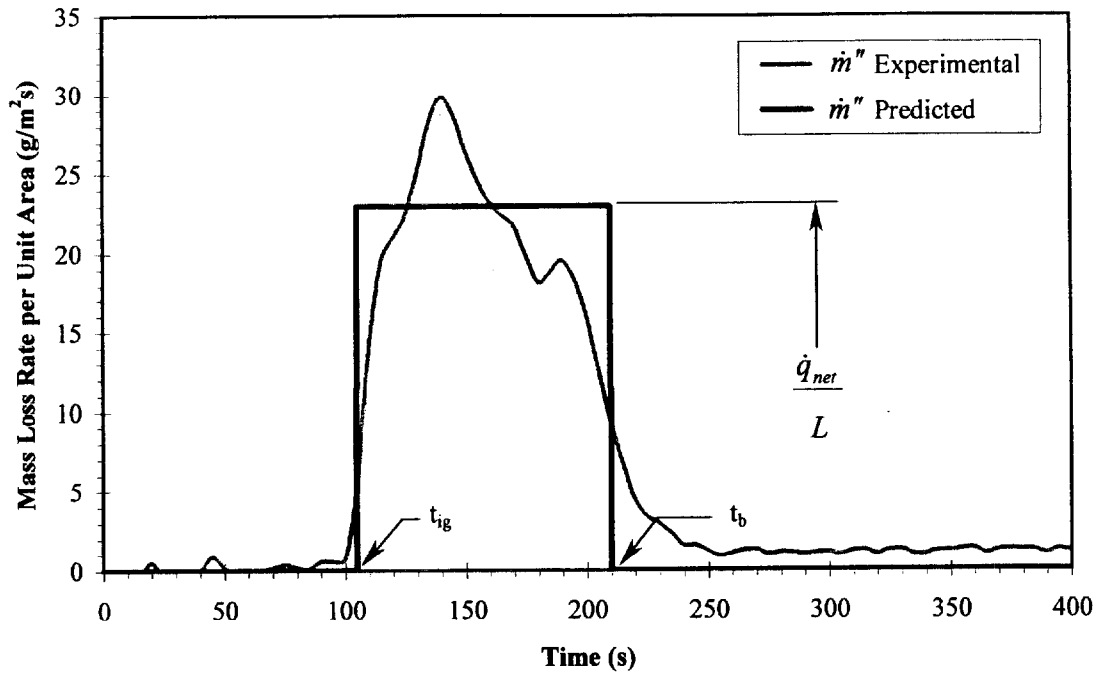


Figure 3. 7: Example of a Typical Burning Rate per Unit Area (\dot{m}'') Prediction: R 4.08, 3-Layer Polycarbonate Panel at 50 kW/m² in the Cone Calorimeter.

Using mass loss rate data from the Cone Calorimeter, estimations of the heat of gasification can be made. This effective L value can then be used to predict the rate of burning of a material over a range of external heat flux values.

The heat of gasification also allows the energy release rate of a material to be predicted. Equation 3.4 indicates that the energy release rate per unit area can be determined by multiplying the mass loss rate per unit area by the heat of combustion thereby allowing Equation 3.6 to be expressed as:

$$\dot{Q}'' = \dot{q}_{net}'' \frac{\Delta H_C}{L} \quad (3.7)$$

where \dot{Q}'' is the energy release rate per unit area of burning material (kW/m²) and ΔH_C is the heat of combustion—as calculated in Section 3.3.2. The predicted energy release

rate will become equal to the right hand side of Equation 3.7 at ignition and remain constant over the burning time. Figure 3.8 shows a comparison of a typical predicted energy release rate versus an actual experimentally measured rate. The predicted energy release rate and burnout time, t_{bo} , are calculated such that the area under the predicted curve, \dot{Q}'' , is equivalent to the area under the experimental curve.

3.4.2 Cone Calorimeter Heat Flux

Equations 3.6 and 3.7 indicate that the mass loss rate and energy release rate per unit area may be linearly dependent on the net heat flux. In the Cone Calorimeter, the net heat flux to the sample is

$$\dot{q}_{net}'' = (1 - \alpha_f) \dot{q}_{ext}'' + \dot{q}_f'' - \dot{q}_{rr}'' \quad (3.8)$$

where α_f is the flame absorptivity, \dot{q}_{ext}'' is the external heat flux provided by the Cone heater (kW/m^2) and \dot{q}_f'' is the total incident heat flux from the flame including both radiant and convective heating (kW/m^2):

$$\dot{q}_f'' = \dot{q}_{f,r}'' + \dot{q}_{f,c}''$$

and \dot{q}_{rr}'' is the heat flux lost due to re-radiation (kW/m^2) from the heated material surface. Therefore, it would be advantageous if the heat flux from the flame, \dot{q}_f'' , and the re-radiant losses, \dot{q}_{rr}'' , can be determined to be constant over a range of external heat fluxes thereby producing a heat of gasification value that is linearly dependent on the external heat flux alone. This linear dependence will allow effective heat of gasification values to be extracted from the Cone data.

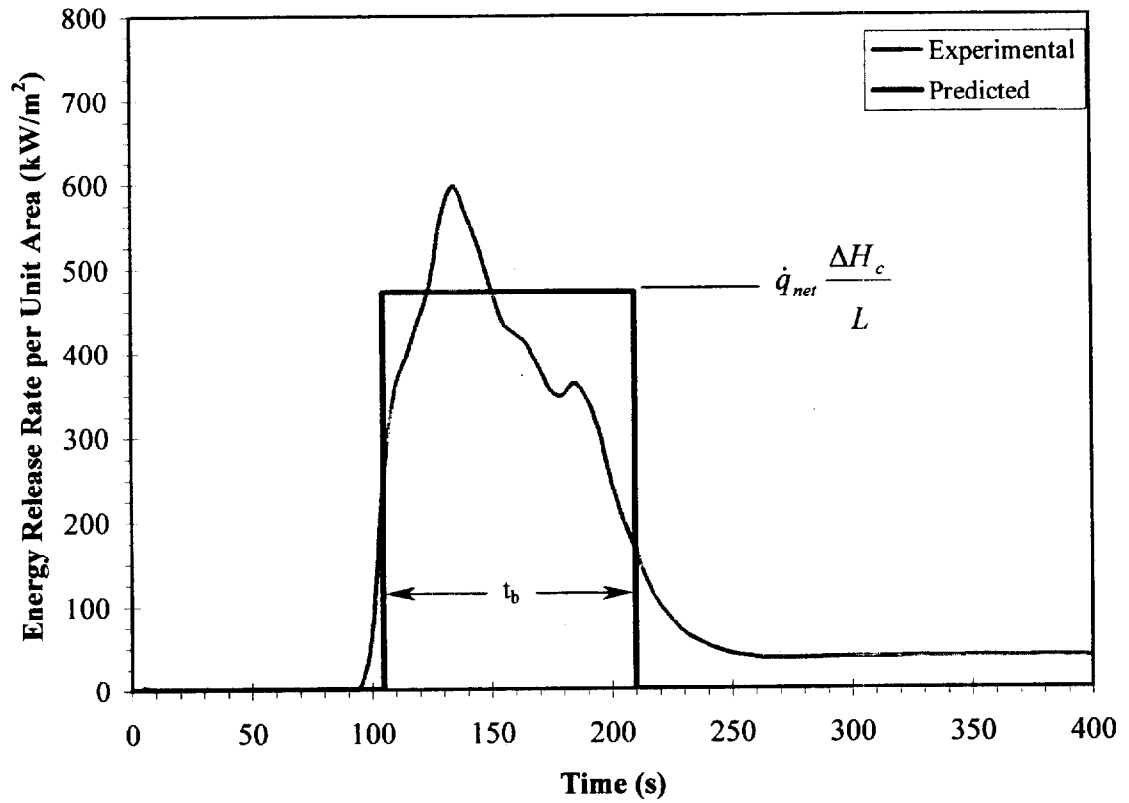


Figure 3. 8: Example of a Typical Energy Release Rate per Unit Area (\dot{Q}'') Prediction: R 4.08, 3-Layer Polycarbonate Panel at 50 kW/m² in the Cone Calorimeter.

Using Kirchhoff's law [20] the absorptivity of the flame can be determined to be equal to the flame emissivity:

$$\alpha_f = \varepsilon_f$$

where ε_f is the emissivity of the flame. Quintiere and Rhodes [42] and Rhodes [43] demonstrated that the flame volume for materials burning in the Cone Calorimeter can be approximated as a tall, vertical cylinder and that the emissivity can be approximated by:

$$\varepsilon_f \cong 1 - e^{-\kappa_f l_m}$$

where κ is the absorption coefficient (m^{-1}) and l_m is the mean beam length (m). For tall, semi-infinite cylindrical flames with height (z) greater than twice the sample width (d), the mean beam length for radiation to the base of the cylinder (the surface of the sample material) is approximately $0.65 \cdot d$ [20]. Therefore for flames of height z greater than $2d$, the flame emissivity is approximately constant and a relatively low value—Rhodes calculates 0.09 for PMMA burning in the Cone Calorimeter. Since the flame emissivity is so low, the flames are very transparent and very little of the external heat flux from the Cone heater is absorbed. Therefore most of the external heat flux is transmitted to the sample.

Quintiere and Rhodes also indicate that the total flame heat flux (\dot{q}''_f) from thermoplastic materials burning in the Cone Calorimeter can be considered to be constant for different external heat fluxes. The radiant portion of the flame heat flux is

$$\dot{q}''_{f,r} = \epsilon_f \sigma T_f^4$$

where σ is the Stefan-Boltzmann constant ($5.670 \times 10^{-11} \text{ kW/m}^2 \cdot \text{K}^4$) and T_f is the flame temperature (K). The average flame volume temperature for a burning material can be considered to be relatively constant resulting in a constant $\dot{q}''_{f,r}$ value. For example, black PMMA burning in the Cone has a constant flame temperature of approximately 1400 K and an associated radiant flame heat flux of approximately 20 kW/m^2 [43]. This does not imply that all materials have identical radiative heat fluxes from the flames, but that for a particular burning material, the radiant heat flux is relatively constant.

Rhodes work also indicates that the convective heat flux to a sample in the Cone Calorimeter is relatively constant as well, but can decrease slightly as the burning rate

increases. An increase in the burning rate will produce a “blocking factor” which acts to effectively reduce the convective heat transfer coefficient (h_c). Rhodes determined a convective heat flux of 15 kW/m² for black PMMA in the Cone, assuming a blocking factor of 1 (the burning rate, \dot{m}'' , approaches 0).

The burning rate of the LSF materials does increase with the external heat flux, however this increase appears to be small enough that this decrease in $\dot{q}''_{f,c}$ can be neglected. Therefore, since both the radiative and convective portions of the flame heat flux are approximately constant for tall flames ($z > 2d$), the net flame heat flux incident to materials burning in the Cone Calorimeter, \dot{q}''_f , can be considered to be constant.

The re-radiant heat losses from the material surface (\dot{q}''_r) can be expressed as

$$\dot{q}''_r = \varepsilon_s \sigma T_s^4$$

where ε_s is the emissivity of the material surface and T_s is the surface temperature of the material (K). For this analysis the surface emissivities of the burning materials are approximated as being equal to 1. Since most materials will either darken, warp, melt and even char when burning, this is a reasonable approximation.

Rhodes work and work done by Hopkins and Quintiere [19] suggests that the surface temperature for burning thermoplastic materials in the Cone is constant. This surface temperature represents the vaporization temperature of the material (T_v) which is approximately constant and can be approximated as being equal to the ignition temperature (T_{ig}). Although the vaporization temperature is slightly higher than the ignition temperature for most thermoplastic materials, this appears to be a reasonable assumption based on the currently available data for thermoplastics. This implies that the reradiation losses from the sample are relatively constant over different external heat